Hydra Radio Access Network (H-RAN): Accurate Estimation Of Reflection Configurations (RCs) for Reconfigurable Intelligent Surfaces (RIS).

Rafid I. Abd
Scho. of Electrical and Electronic Eng.
Yonsei University
Seoul 03722, South Korea
Email address: Rafid@yonsei.ac.kr

Kwang Soon Kim
Scho. of Electrical and Electronic Eng.
Yonsei University
Seoul 03722, South Korea
Email address: ks.kim@yonsei.ac.kr

Junxiu Han
Scho. of Electrical and Electronic Eng.
Yonsei University
Seoul 03722, South Korea
Email address: junxiu@yonsei.ac.kr

***Abstract*—The necessity for a cohesive network that seamlessly integrates various networks, technologies, and services is becoming increasingly pressing. By adopting innovative networking solutions that unify these disparate networks, Hydra radio access networks (H-RANs) embody a forward-looking approach that is essential for navigating the complexities of the evolving digital landscape. By integrating advanced communication and sensing capabilities, as well as harnessing the power of artificial intelligence/machine learning (AI/ML), H-RANs are set to redefine how services are delivered and managed within modern telecommunications networks. This comprehensive strategy ensures that these networks are not only current but also poised for future innovations. Concurrently, reconfigurable intelligent surfaces (RISs) are envisioned as programmable surface structures that control electromagnetic wave reflection, thereby modifying the wireless communication environment. Despite their advantages, a major challenge for RIS technology lies in the high overhead associated with beam alignment and channel estimation for MMW systems. These conventional methods require extensive pilot signaling to estimate channel state information (CSI) accurately, leading to significant computational and operational burdens. This study proposes a novel approach to accurately estimate RIS's reflection configurations (RCs) using real-time sensor data extracted from sensor and radio units (SRUs) and AI/ML D-engine. This method aims to enhance RIS functionality by providing precise information that allows dynamic adjustments to RCs. Simulations demonstrate that our approach significantly boosts network performance, achieving high selection accuracy by achieving a remarkable 95% selection accuracy using only five RC index candidates.**

***Index Terms*—Hydra radio access network (H-RAN), Multi-functional networks, Perceptive networks, Heterogeneous data, AI/ML engines, Cooperative multi-sparse input/multi-task learning-based federated learning (C-SMTL), Reconfigurable intelligent surfaces (RISs), Reflection configurations (RCs).**

This work was partly supported by Institute of Information & communications Technology Planning & Evaluation (IITP) grant funded by the Korea government (MSIT) (No.RS-2024-00397216, Development of the Upper-mid Band Extreme massive MIMO(E-MIMO), 50%) and the National Research Foundation of Korea (NRF) grant funded by the Korea government (MSIT) (No.2022R1A5A1027646, Augmented Cognition Meta-Communications Research Center, 50%.

I. Introduction

Indeed, conventional radio access networks (RANs) struggle to adapt to rapid and frequent changes in network environments due to their inherent limitations. They often rely on (a one-size-fits-all solution), which is static solutions and lacks the sophisticated perceptive capabilities provided by modern technologies, such as AI and sensors. This results in a rigid approach that cannot effectively address the nuanced and dynamic nature of current networking demands [1], [2]. Hydra radio access network's (H-RAN's) vision is centered around the unification of diverse networks and technologies, encompassing communication networks, sensor networks, edge computing (EC), the internet of things (IoT), artificial intelligence/machine learning (AI/ML), autonomous driving (AD), vehicle-to-everything (V2X), etc. Ultimately, the development of H-RANs as a cohesive operational framework not only addresses current technological needs but also prepares the infrastructure for future advancements. By fostering an adaptable environment that leverages cutting-edge technologies, H-RANs position themselves to support the continued evolution of wireless communication and connectivity solutions [1], [2]. Moreover, incorporating dense sensor and radio units (SRUs) within the H-RAN framework is essential for developing dynamic and responsive networks capable of adapting to modern connectivity needs. This is particularly vital as technological advancements continue to push the limits of network demands and expectations, particularly in challenging millimeter-wave (MMW) environments [1]–[3]. MMW systems are characterized by significant propagation losses which can be attributed to their high carrier frequencies. In addition to propagation losses, MMW systems are highly vulnerable to blockages caused by physical obstructions [3]–[5]. On the other hand, reconfigurable intelligent surfaces (RISs) are developed as programmable surface structures that control electromagnetic wave reflection, thereby modifying the wireless communication environment [6]–[8]. They achieve

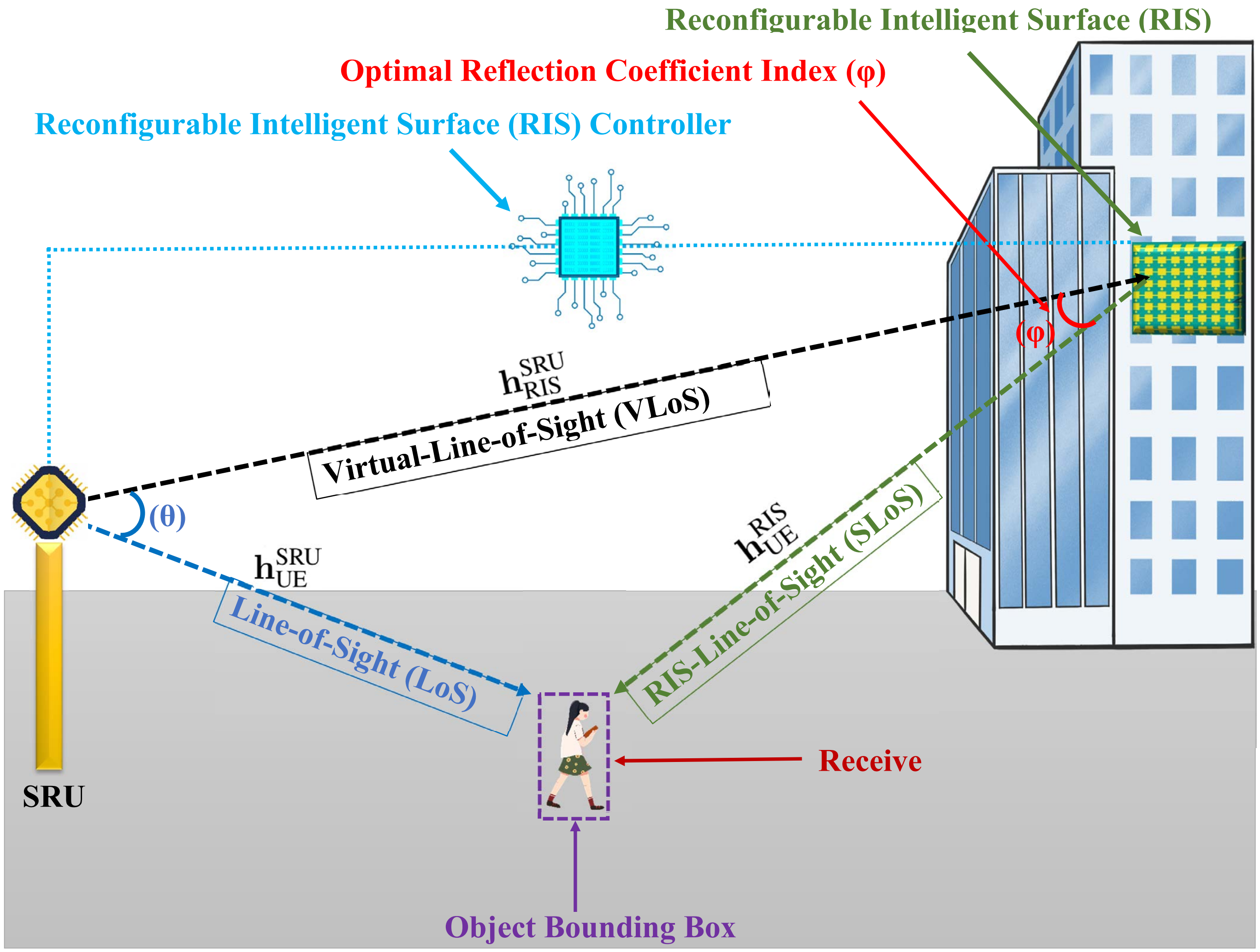

Figure 1: Hydra radio access networks (H-RAN) incorporate disaggregated sensor and radio units (SRUs) and reconfigurable intelligent surfaces (RISs), streamlining heterogeneous network deployments. In these scenarios, the sensor data, including parameters like location, allows SRUs to assess the current state of the wireless channel and make informed decisions about the RIS configuration. The Hydra distributed unit (H-DU) only needs feedback on the optimal phase configuration index to the RIS through the control link of the corresponding SRU. With the capability to reconfigure the RIS based on real-time sensor data, H-RAN can enhance propagation conditions.

this by adjusting the electric and magnetic properties of the surface, allowing for enhanced signal steering towards intended receivers. While RIS technology promises significant performance enhancements in MMW systems, making precise beam alignment essential but challenging. Traditional beam alignment and channel estimation methods present a considerable challenge due to their high overhead, particularly in dynamic environments where rapid CSI updates are required [6]–[8]. This study proposes a novel approach to accurately select the optimal reflection configurations (RCs) on RIS using real-time sensor data extracted from SRUs. This method aims to enhance RIS functionality by providing precise information that allows dynamic adjustments to RCs through the AI/ML D-engine [1], [2]. Simulations demonstrate that our approach significantly enhances network performance, approaching high selection accuracy. Furthermore, it achieves a remarkable 95% RC selection accuracy while maintaining high efficiency.

II. Network Model

In this paper, an RIS-aided H-RAN communication system is investigated. As shown in Fig. 1, we consider an outdoor H-RAN framework in which single-access cellular networks of SRU are used, as well as RIS-aided multiple-input and single-output communication systems, and an RIS controller. SRUs are an integral part of H-RAN architectures, extending their functionality beyond traditional communication tasks. They serve as critical nodes that integrate sensing and communication capabilities. This dual capability enables the network to process and analyze sensor data while facilitating reliable wireless communication to the adaptive and responsive network environment [1], [2]. A single SRU can provide valuable insights into the UE's status, e.g., location, distance, velocity, signal conditions, etc., enabling the network to assess and respond to changes in real time. Meanwhile, as shown in Fig. 1, we consider a RIS-assisted communication system with N reflecting elements $\mathbf{N} = \{1, 2, \ldots, N\}$ to assist in downlink communication from an SRU with M antennas $\mathbf{M} = \{1, 2, \ldots, M\}$ to single-antenna user equipment (UE). The SRU antenna arrays and the RIS reflecting elements are modeled as uniform linear arrays (ULA). The reflective elements of the RIS are each connected to an atom that adjusts the phase of each incident wave. To simplify the description of the system, the positions of the BS, the RIS, and the UE are indicated by a Cartesian coordinate system. The UE position is extracted by SRU and represented by $\mathbf{p} = (p_x, p_y, p_z)^{\mathrm{T}}$. We assume that an SRU or collaborative SRU transmits UE status information directly to the RIS through a control link. In addition, it is assumed that the RIS phase shifts are estimated by the Hydra distributed unit (H-DU) and transmitted to the RIS controller via dedicated control channels [1], [2]. The H-DU employs a hybrid precoding configuration, where each RF chain is adapted to all available antennas, and transmits Gaussian data symbols $\mathbf{s} = [s_1, \ldots, s_K]^{\mathrm{T}} \in \mathbb{C}^{K\times 1}$ to the users via a digital and analog precoding matrix.

Assuming the uplink transmission signal has a symbol $s \in \mathbb{C}$, therefore, the received signal at the SRU after combining can be written as

$$y = \mathbf{w}^H \mathbf{h} s + \mathbf{w}^H \mathbf{n}, \tag{1}$$

where $\mathbb{E}\left[|s|^2\right] = P_s$ is the transmitted symbol that satisfies the average power constraint, $\mathbf{n} \sim \mathcal{N}_{\mathbb{C}}\left(0, \sigma_n^2 \mathbf{I}\right)$ is the received noise vector at the SRU, $\mathbf{h} \in \mathbb{C}^{M\times 1}$ denotes the uplink channel between the UE and the SRU, and w indicates the SRU combining vector.

A. Channel Model

In addition, each RIS element is connected to a smart RIS controller, which can independently adjust the phase of incident signals. Furthermore, given the practical hardware implementation, we presume the discrete phase shift of $\{0, 2\pi\}$ which is uniformly quantified by each RIS element. For each element, let $\{\chi\}$ refer to the number of quantization bits. Accordingly, we have reflection coefficient (RC) matrices set $\Theta = \{e^{j0}, e^{j\Delta\theta}, \ldots, e^{j(2^q-1)\Delta\theta}\}$, where $\Delta\theta = \{2\pi/2^\chi\}$ denotes the quantified interval. Let $\Gamma = \{\Gamma_1, \Gamma_2, \ldots, \Gamma_N\}^T \in \mathbb{C}^{N\times 1}$ represent the RC vector, where $\Gamma_n \in \Gamma$, $n \in \mathbf{N}$ refer to the RC of the n_{th} RIS element. Let $\mathbf{\Gamma} = \mathrm{diag}(\{\Gamma_1, \Gamma_2, \ldots, \Gamma_N\}) \in \mathbb{C}^{N\times N}$ denote the reflection matrix of the RIS. Let $\mathrm{h}_{\mathrm{UE}}^{\mathrm{SRU}} \in \mathbb{C}^{1\times\mathrm{M}}$ $\mathrm{h}_{\mathrm{RIS}}^{\mathrm{SRU}} \in \mathbb{C}^{\mathrm{M}\times\mathrm{R}}$, and $\mathrm{h}_{\mathrm{UE}}^{\mathrm{RIS}} \in \mathbb{C}^{1\times\mathrm{N}}$ denote the complex baseband channel from the SRU $\rightarrow$ UE, from the SRU $\rightarrow$ RIS, and from the RIS $\rightarrow$ UE, respectively. The Rician channel model [6] is used to characterize wireless communication environments where the received signal consists of a dominant LoS component, along with multiple scattered NLoS components. This model is particularly applicable in scenarios where a strong direct path exists between the transmitter and receiver. The direct channel SRU $\rightarrow$ UE $\mathrm{h}_{\mathrm{UE}}^{\mathrm{SRU}} \in \mathbb{C}^{1\times\mathrm{M}}$ is generated by

$$\mathrm{h}_{\mathrm{UE}}^{\mathrm{SRU}} = \sqrt{P_1/\left(K_1+1\right)}\left(\sqrt{K_1}\mathrm{h}_{\mathrm{UE}\ (\mathrm{LoS})}^{\mathrm{SRU}} + \mathrm{h}_{\mathrm{UE}\ (\mathrm{NLoS})}^{\mathrm{SRU}}\right), \tag{2}$$

where $\mathrm{h}_{\mathrm{UE}\ (\mathrm{LoS})}^{\mathrm{SRU}}$ and $\mathrm{h}_{\mathrm{UE}\ (\mathrm{NLoS})}^{\mathrm{SRU}}$ are the LoS and NLoS components of $\mathrm{h}_{\mathrm{UE}}^{\mathrm{SRU}}$, respectively. The NLoS component is modeled by a complex Gaussian distribution $\mathrm{h}_{\mathrm{UE}}^{\mathrm{SRU}}(\mathrm{NLoS}) \sim \mathcal{N}_{\mathbb{C}}\left(0, \sigma n^2 \mathbf{I}\right)$. $P\mathrm{L}$ and K_{d} denote the path loss and Rician factor of the direct channel SRU $\rightarrow$ UE, respectively. Likewise, the channels SRU $\rightarrow$ RIS ($\mathrm{h}_{\mathrm{RIS}}^{\mathrm{SRU}}$) and RIS $\rightarrow$ UE ($\mathrm{h}_{\mathrm{UE}}^{\mathrm{RIS}}$) are generated similarly to (2).

$$\begin{cases} \mathrm{h}_{\mathrm{RIS}}^{\mathrm{SRU}} = \{\sqrt{P_2/\left(K_2+1\right)}\left(\sqrt{K_2}\mathrm{h}_{\mathrm{RIS(LoS)}}^{\mathrm{SRU}} + \mathrm{h}_{\mathrm{RIS(NLoS)}}^{\mathrm{SRU}}\right)\}, \\ \mathrm{h}_{\mathrm{UE}}^{\mathrm{RIS}} = \{\sqrt{P_3/\left(K_3+1\right)}\left(\sqrt{K_3}\mathrm{h}_{\mathrm{UE\ (LoS)}}^{\mathrm{RIS}} + \mathrm{h}_{\mathrm{UE\ (NLoS)}}^{\mathrm{RIS}}\right)\}, \end{cases} \tag{3}$$

Accordingly, this complex downlink channel $\hat{\mathbf{h}}$ can be expressed as

$$\begin{aligned} \hat{\mathbf{h}} &= \mathbf{h}_{\mathrm{UE}}^{\mathrm{SRU}} + \mathbf{h}_{\mathrm{RIS}}^{\mathrm{SRU}}\Gamma\mathbf{h}_{\mathrm{UE}}^{\mathrm{RIS}} \\ &= \mathbf{h}_{\mathrm{UE}}^{\mathrm{SRU}} + \mathbf{h}_{\mathrm{RIS}}^{\mathrm{SRU}}\Gamma^T \mathrm{diag}(\mathbf{h}_{\mathrm{UE}}^{\mathrm{RIS}})' \end{aligned} \tag{4}$$

where $\mathbf{h}_{\mathrm{UE}}^{\mathrm{SRU}} \in \mathbb{C}^{\mathrm{M}\times 1}$, $\mathbf{h}_{\mathrm{RIS}}^{\mathrm{SRU}} \in \mathbb{C}^{\mathrm{M}\times\mathrm{N}}$, and $\mathbf{h}_{\mathrm{UE}}^{\mathrm{RIS}} \in \mathbb{C}^{\mathrm{N}\times 1}$, indicate the channel from the SRU to the UE, from the SRU to the RIS, and finally from the RIS to the UE, respectively. $\mathbf{\Gamma} = \mathrm{diag}(\{\Gamma_1, \Gamma_2, \ldots, \Gamma_N\}) \in \mathbb{C}^{N\times N}$ refer to the RIS reflection matrix which can be formulated as

$$\Gamma = \mathrm{diag}\left(A_1 e^{(j\theta_1)}, A_2 e^{(j\theta_2)}, \ldots, y_{\mathrm{n}} e^{(j\theta_n)}\right), \tag{5}$$

where $\theta_n \in (0, 2\pi)$ and $A_n \in (0, 1)$ correspond to the phase-shift and the amplitude coefficient for element $n \in (1, 2, \ldots, n)$, respectively. During signal reflection, when an incoming signal $\mathbf{s}$ impinges on the RIS, the reflected signal $\mathbf{r}$ can be described by

$$\mathbf{r} = \Gamma\mathbf{s}, \tag{6}$$

where $\mathbf{s}$ is the vector of the incoming signal components at each RIS element. and $\mathbf{r}$ is the vector of the reflected signal components.

III. SRU And RIS Steering Vectors.

In this section, we illustrate an innovative approach that leverages sensor data in SRU to estimate accurate RCs for RIS. SRU can provide scene understanding and precise information about the environment, including distances and relative positions of objects, and distinguish between different types of surfaces (e.g., reflective, absorption). The data collected from SRU sensors can be analyzed to determine incidence and reflection angles for incoming signals. The estimated RCs derived from sensor data can be simulated to assess their effectiveness in improving signal quality. This entails analyzing incidence and reflection angles to optimize signal paths within the communication environment. We estimated the optimal beam index for direct channel SRU $\rightarrow$ UE ($\mathrm{h}_{\mathrm{UE}}^{\mathrm{SRU}} \in \mathbb{C}^{1\times \mathrm{M}}$) and SRU $\rightarrow$ RIS ($\mathrm{h}_{\mathrm{RIS}}^{\mathrm{SRU}} \in \mathbb{C}^{\mathrm{M}\times \mathrm{R}}$) according to our previous study in [2]. In this approach, the H-RAN draws upon sensor data collected by SRU to define a small set of candidate beams at the transmitter, each pointing in a certain direction. Beam directions are dynamically generated based on detected UEs' positions and orientations. let $\mathbf{a}_{\mathrm{RIS}\ (\psi)}^{\mathrm{SRU}} \in \mathbb{C}^{M\times 1}$ denote the steering vector of the SRU with m_{th} elements SRU $\rightarrow$ RIS ($\mathrm{h}_{\mathrm{RIS}}^{\mathrm{SRU}} \in \mathbb{C}^{\mathrm{M}\times \mathrm{R}}$) which can be expressed as

$$\mathbf{a}_{\mathrm{RIS}\ (\psi)}^{\mathrm{SRU}} = e^{j2\pi(m-1)\mathrm{d}_{\mathrm{SRU}}\sin\psi/\lambda}, \tag{7}$$

where $\mathrm{d}_{(\mathrm{SRU})}$ and λ denote the antenna spacing and the wavelength of the signal in the SRU, respectively, with an angel range from $\psi \in [-\pi/2, \pi/2)$. Moreover, let $\mathbf{a}_{\mathrm{UE}\ (\varphi,\gamma)}^{\mathrm{RIS}} \in \mathbb{C}^{N\times 1}$ denotes the steering vector from RIS $\rightarrow$ UE, which can be formulated as [6]

$$\mathbf{a}_{\mathrm{UE}\ (\varphi,\gamma)}^{\mathrm{RIS}} = e^{j2\pi \mathrm{d}_{\mathrm{RIS}}\sin\gamma} \left[\lfloor\frac{n-1}{\mathrm{N}_{\mathrm{RIS}}}\rfloor \sin\varphi + \left((n-1) - \lfloor\frac{n-1}{\mathrm{N}_{\mathrm{RIS}}}\rfloor \mathrm{N}_{\mathrm{RIS}}\right)\cos\varphi\right]/\lambda, \tag{8}$$

where d is antenna spacing and the and λ is the wavelength. $\varphi \in [0, \pi)$, and $\gamma \in [-\pi/2, \pi/2)$ indicate the azimuth and elevation (AoA/AoD), accordingly. $\mathrm{d}_{\mathrm{RIS}}$, and $\mathrm{N}_{\mathrm{RIS}}$ are the element spacing, and the number of reflecting elements placed at each row of the RIS, respectively. Therefore, LoS components of the SRU $\rightarrow$ UE ($\mathrm{h}_{\mathrm{UE}}^{\mathrm{SRU}}$), SRU $\rightarrow$ RIS ($\mathrm{h}_{\mathrm{RIS}}^{\mathrm{SRU}}$), and RIS $\rightarrow$ UE ($\mathrm{h}_{\mathrm{UE}}^{\mathrm{RIS}}$) can be formulated as a function of steering vectors for [$\mathbf{a}_{\mathrm{UE}}^{\mathrm{SRU}}(\phi_{\mathrm{UE}}^{\mathrm{SRU}})$], [$\mathbf{a}_{\mathrm{RIS}}^{\mathrm{SRU}}$ ($\varphi_{\mathrm{RIS}}^{\mathrm{SRU}}, \gamma_{\mathrm{RIS}}^{\mathrm{SRU}}$) $\mathbf{a}_{\mathrm{RSI}}^{\mathrm{SRU}}(\phi_{\mathrm{RSI}}^{\mathrm{SRU}})$], and [$\mathbf{a}_{\mathrm{UE}}^{\mathrm{RIS}}$ ($\varphi_{\mathrm{UE}}^{\mathrm{RIS}}, \gamma_{\mathrm{UE}}^{\mathrm{RIS}}$)] respectively [6]–[8]. Here ($\phi_{\mathrm{UE}}^{\mathrm{SRU}}$) and ($\phi_{\mathrm{RIS}}^{\mathrm{SRU}}$) represent the AoA from the SRU $\rightarrow$ UE and the AoD from the SRU $\rightarrow$ RIS, respectively, where ($\varphi_{\mathrm{RIS}}^{\mathrm{SRU}}$) and ($\gamma_{\mathrm{RIS}}^{\mathrm{SRU}}$) indicate the azimuth and elevation AoA from the SRU $\rightarrow$ RIS, correspondingly, where ($\varphi_{\mathrm{UE}}^{\mathrm{RIS}}$), and ($\gamma_{\mathrm{UE}}^{\mathrm{RIS}}$) denote the azimuth and elevation AoA from the RIS $\rightarrow$ UE, accordingly.

A. RIS-Based Beamforming Configuration

In this section, we propose a RIS beam selection model that uses SRU multimodal data to identify a small subset of candidate beams, which SMTL subsequently trains to select the beam that maximizes the normalized signal power [28]. More specifically, the main algorithmic component involves amounts to proposing a means for identifying a small subset of possible phase shift configurations for the RIS, where each configuration is a vector of phase shifts applied to the RIS elements $\mathcal{P}_k \subseteq \mathcal{P}$ of K beam pairs such that $(i^*, j^*) \in \mathcal{P}_k$ with high probability. To do so, we assume a fixed RIS codebook $\mathcal{C}_{\mathrm{RIS}} = \{\boldsymbol{\phi}_1, \boldsymbol{\phi}_2, \ldots, \boldsymbol{\phi}_{M_i}\}$, $\mathcal{C}_{\mathrm{RIS}} = \{\boldsymbol{\phi}_i\}_{i=1}^{C_{\mathrm{RIS}}}$, where each $\boldsymbol{\phi}_i$ represents a different phase shift configuration for the RIS. Also, we assume a fixed receiver codebook $\mathcal{C}_{\mathrm{UE}} = \{\mathbf{w}_1, \mathbf{w}_2, \ldots, \mathbf{w}_{M_j}\}$, $\mathcal{C}_{\mathrm{UE}} = \{\mathbf{w}_j\}_{j=1}^{C_{\mathrm{UE}}}$, where each $\mathbf{w}_j$ represents a different beamforming vector for the receiver. Therefore, we seek to achieve certain indexes containing the corresponding best beam pair labels at the RIS and receiver sides with the definition of $(i^*, j^*) \in \mathcal{C}_{\mathrm{RIS}} \times \mathcal{C}_{\mathrm{UE}}$.

Assuming that the RIS steers the signal from the SRU to the UE, the overall received signal at the receiver after considering the i_{th} configuration of the RIS and the j_{th} beamforming vector can be written as

$$y_{(i,j)} = \mathbf{w}_j^H \left(\mathrm{h}_{\mathrm{UE}}^{\mathrm{SRU}}\mathrm{H}_{\mathrm{UE}}^{\mathrm{RIS}} + \mathrm{h}_{\mathrm{RIS}}^{\mathrm{SRU}}\boldsymbol{\phi}_i \mathbf{h}_{\mathrm{UE}}^{\mathrm{RIS}}\right) s + \mathbf{w}_j^H \mathbf{n}, \tag{9}$$

where $\mathrm{h}_{\mathrm{UE}}^{\mathrm{SRU}}$ represents a direct channel from the SRU $\rightarrow$ UE, $\mathrm{H}_{\mathrm{UE}}^{\mathrm{RIS}}$ is a channel vector from the RIS $\rightarrow$ UE, $\mathrm{h}_{\mathrm{RIS}}^{\mathrm{SRU}}$ refers to the channel vector from the SRU $\rightarrow$ RIS, $\mathbf{h}_{\mathrm{UE}}^{\mathrm{RIS}}$ indicates combined channel matrix from the RIS $\rightarrow$ UE.

This approach aims to maximize the received signal power by finding the optimal pair $(\boldsymbol{\phi}_i^*, \mathbf{w}_j^*)$ that maximizes the received signal power

$$(\boldsymbol{\phi}_i^*, \mathbf{w}_j^*) = \underset{1\le m\le M, 1\le n\le N}{\arg\max} \left|\mathbf{w}_j^H \left(\mathrm{h}_{\mathrm{UE}}^{\mathrm{SRU}}\mathrm{H}_{\mathrm{UE}}^{\mathrm{RIS}} + \mathrm{h}_{\mathrm{RIS}}^{\mathrm{SRU}}\boldsymbol{\phi}_i \mathbf{h}_{\mathrm{UE}}^{\mathrm{RIS}}\right)\right|^2, \tag{10}$$

for each pair $(\boldsymbol{\phi}_i, \mathbf{w}_j)$, we can compute the received signal power $P_{i,j}$, and identify the pair $(\boldsymbol{\phi}_i, \mathbf{w}_j)$ that maximizes the signal power as

$$(\boldsymbol{\phi}_i^*, \mathbf{w}_j^*) = \underset{i,j}{\arg\max} \left|\mathbf{w}_j^H \left(\mathrm{h}_{\mathrm{UE}}^{\mathrm{SRU}}\mathrm{H}_{\mathrm{UE}}^{\mathrm{RIS}} + \mathrm{h}_{\mathrm{RIS}}^{\mathrm{SRU}}\boldsymbol{\phi}_i \mathbf{h}_{\mathrm{UE}}^{\mathrm{RIS}}\right)\right|^2, \tag{11}$$

For additional simplification, we can further break down the computation for each i in $\mathcal{C}_{\mathrm{RIS}}$ and j in $\mathcal{C}_{\mathrm{UE}}$ as follows

$$\mathbf{v}_{(i,j)} = \mathbf{w}_j^H \mathrm{h}_{\mathrm{RIS}}^{\mathrm{SRU}} \boldsymbol{\phi}_i \mathbf{h}_{\mathrm{UE}}^{\mathrm{RIS}}, \tag{12}$$

By adding the direct channel contribution, we can formulate an equation as

$$\mathbf{u}_{(i,j)} = \mathbf{v}_{(i,j)} + \mathbf{w}_j^H \mathrm{h}_{\mathrm{UE}}^{\mathrm{SRU}} \mathrm{H}_{\mathrm{UE}}^{\mathrm{RIS}}, \tag{13}$$

Therefore, the signal power for each configuration can be computed as

$$P_{(i,j)} = \left|\mathbf{u}_{(i,j)}\right|^2, \tag{14}$$

As a result, we can formulate the maximum selection from the configuration $(\boldsymbol{\phi}_i^*, \mathbf{w}_j^*)$ that gives the maximum $P_{(i,j)}$. Therefore, the signal-to-noise ratio (SNR) for a given RIS configuration $\boldsymbol{\phi}_i$ and receiver beamforming vector $\mathbf{w}_j$ can be expressed as

$$\mathrm{SNR}_{i,j} = \frac{\left|\mathbf{w}_j^H \left(\mathrm{h}_{\mathrm{UE}}^{\mathrm{SRU}}\mathrm{H}_{\mathrm{UE}}^{\mathrm{RIS}} + \mathrm{h}_{\mathrm{RIS}}^{\mathrm{SRU}}\boldsymbol{\phi}_i \mathbf{h}_{\mathrm{UE}}^{\mathrm{RIS}}\right)\right|^2}{\sigma_n^2}, \tag{15}$$

where σ_n^2 is the noise power. Accordingly, we can maximize the SNR by selecting the optimal pair $(\boldsymbol{\phi}_i, \mathbf{w}_j)$ from their respective codebooks as

$$(\boldsymbol{\phi}_i^*, \mathbf{w}_j^*) = \underset{i,j}{\arg\max}\, \mathrm{SNR}_{i,j}, \tag{16}$$

IV. Cooperative Multi-Sparse Input/Multi-Task Learning-Based Federated Learning (C-SMTL)

The one-size-fits-all approach commonly adopted by traditional RANs does not adequately meet the specific needs of different applications. This generalization can lead to inefficiencies, as the diverse nature of communication tasks often requires tailored solutions that consider individual application requirements, and real-time communication environment conditions. The SMTL is developed to overcome this limitation by learning a function that maps from the multi-input sample space to multi-output spaces, where each output addresses a particular objective. SMTL can perform multiple tasks simultaneously during training, where each task has a specific set of labeled data, and the model learns to perform all tasks simultaneously. The input to the SMTL model is divided into several groups, each of which corresponds to a specific observation of input features. In each group, the input features for the neural network are derived from observations gathered at that particular point in time. For each group, the model produces task-specific outputs incorporating the observed input features and the learned representations captured by the H-RAN network. In this paper, SMTL-DRL is designed to adapt to the dynamic environment and make real-time decisions to select optimal RCs.

A. C-SMTL-Based RIS Beam Selection Scheme

We formulated the selection of the optimal beam pair vectors at the RIS and UE as a decision-making problem. Deep Reinforcement Learning (DRL) is well-suited to such tasks, where the goal is to learn a policy that selects beam pairs that maximize a certain reward (e.g., the received signal power and SNR) [9]–[11]. First, we represent the current state of the system s_t, which includes information about channel condition, sensor data, previous beam selections, etc. Second, the action a_t is defined as selecting a beam pair vector (e.g., selecting a beamforming vector at the UE and a phase configuration at the RIS). Third, the reward function r_t, typically expressed as the (e.g., received signal power, or SNR) after taking action a_t in a state s_t. Finally, we formulate the policy $\pi(a_t|s_t)$ which refers to the probability of taking action a_t under the given state s_t. C-SMTL-DRL is designed to learn a policy π^* that optimizes the expected cumulative reward (i.e., the expected sum of rewards over time

$$\pi^* = \arg\max_{\pi} \mathbb{E}\left[\sum_{t=0}^{T} \gamma^t r_t\right], \tag{17}$$

where $\gamma \in [0, 1)$ refers to the discount factor and T indicates the time horizon.

In the action a_t setting, in each time step t, the C-SMTL-DRL agent (e.g., deep Q-network (DQN), deep deterministic policy gradient (DDPG), etc.) selects an action (beam pair) based on the current state s_t

$$a_t = \arg\max_{a} Q(s_t, a; \theta), \tag{18}$$

where $Q(s_t, a; \theta)$ is the Q-value function that estimates the expected cumulative reward r_t for taking action a_t in-state s_t, parameterized by θ which indicate the weights of the deep learning neural network.

In this setting, we define the reward function r_t as a function of the SNR

$$r_t = \log_2\left(1 + \frac{\left|\mathbf{w}_j^H\left(\mathrm{h}_{\mathrm{UE}}^{\mathrm{SRU}}\mathrm{H}_{\mathrm{UE}}^{\mathrm{RIS}} + \mathrm{h}_{\mathrm{RIS}}^{\mathrm{SRU}}\phi_i\mathbf{h}_{\mathrm{UE}}^{\mathrm{RIS}}\right)\right|^2}{\sigma_n^2}\right), \tag{19}$$

B. C-SMTL- DRL Optimization Process

The initialization of the optimization process starts by using the replay buffer D to store experiences (s_t, a_t, r_t, s_{t+1}), and initializing the Q-network $Q(s, a; \theta)$ with weights θ. For each episode, we initialize the state s_0 at each time step t and select an action a_t by using an epsilon-greedy policy (with probability ϵ of taking a random action; otherwise, selecting $arg\max_a Q(s_t, a; \theta)$. We implemented the selected action a_t (i.e., selected a beam pair). Next, observe the reward r_t and the next state s_{t+1}. The C-SMTL-DRL records the transition (s_t, a_t, r_t, s_{t+1}) to the replay buffer D. The Q-network is updated by sampling a random mini-batch of transitions (s_i, a_i, r_i, s_{i+1}) from D and updating the Q-network by minimizing loss.

$$\begin{aligned} L(\theta) = \mathbb{E}_{(s_i,a_i,r_i,s_{i+1})\sim D} \\ \left[\left(r_i + \gamma \max_{a'} Q(s_{i+1}, a'; \theta') - Q(s_i, a_i; \theta)\right)^2\right], \end{aligned} \tag{20}$$

where θ are the weights of the target network, which are periodically updated from θ. Similarly, the state s_t is updated, set $s_t \leftarrow s_{t+1}$. Finally, the above steps repeat until convergence, where the policy $\pi(a_t|s_t)$ consistently selects the beam pairs that maximize the reward.

V. Simulation And Results

In this section, simulations are performed to evaluate the performance of the proposed model using different computational methods, e.g., DeepSense 6G dataset, scenario 35 [12], InSite ray-tracing software [13], and the Python programming platform. Additionally, to train and assess the model, OpenAI Gym [14] is used as an environment template, integrated with Python TensorFlow. OpenAI Gym and TensorFlow offer the necessary tools for implementing complex neural network architectures and APIs for easily creating custom tasks. OpenAI Gym also provides standard benchmark tasks for evaluating different neural network architectures. To determine the converged reward, we sum the latest 20 iterations from M = 200 iterations. We simulate an outdoor H-RAN scenario where one SRU is positioned alongside the road at (x_i, y_i, z_i) and provides a direct link to the RIS and UEs with a random distribution of user densities. This area also has a RIS located at (x_r, y_r, z_r) which provides an indirect link to the UEs. In the simulation, we assume SRU's transmit power is 25 dBm. The duration of periodic feedback t_i reported by SRU_i, includes the UE_j information e.g., position $\mathbf{X}_j(x_j, y_j)$, and the distance between SRU_i and UE_j $\mathbf{D}_j(d_{\mathrm{j,x}}, d_{\mathrm{j,y}})$. Fig. 2 illustrates the comparison of H-RAN performance against to benchmark scheme of RIS-based random phase, in which the phase shifts are randomly chosen from $(0, 2\pi]$, whereas the beamforming matrix is obtained as where each $\Gamma_i = e^{j\theta_i}$ with $\theta_i \sim \mathrm{Uniform}(0, 2\pi]$ for used number of RCs as a selection accuracy. Simulation results show that the proposed model outperforms the existing ones in terms of accuracy and robustness. Furthermore, the results indicate that the proposed model suits large-scale networks. This is because by analyzing the sensor data, the system can determine the positions of the RIS and receivers. This spatial information can then be used to calculate the phase shifts that align the reflected beams toward the receiver, thereby maximizing signal strength.

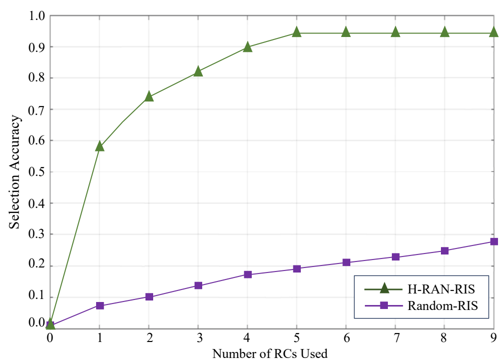

Figure 2: Number of RCs used as a function of selection accuracy.

VI. CONCLUSIONS

The evolution towards H-RAN necessitates a holistic approach, wherein various advanced technologies and communication paradigms are integrated into a unified framework. This approach aims to harmonize a variety of components such as wireless access networks, sensors, AI, backhaul solutions, and computing resources, thereby facilitating seamless connectivity and service delivery across diverse applications. The integration of these technologies fosters a cohesive operational framework capable of addressing the demands of modern applications. SMTL framework is engineered to select tasks specifically tailored to meet particular network conditions. This framework's adaptability allows for swift adjustments to network conditions fluctuations, thus enhancing overall network responsiveness. However, beam alignment is a critical challenge when implementing RIS technology due to the intricacies introduced by multiple controllable elements within RIS. In addition, the challenge of high overhead associated with conventional channel estimations in RIS may detract from the performance benefits of this technology. To address this limitation, we propose a novel solution through the implementation of a sensor information-assisted beamforming design that offers a viable solution that eliminates the need for extensive channel training processes, thus enhancing decision-making for AI/ML D-engines, which rely on access to accurate and timely data. The objective is to control the RIS elements such that the reflected beam is directed toward a desired target. This is done by optimizing the phase shifts of the RIS elements to ensure constructive interference at the desired receiver location. Simulation results reveal that H-RANs significantly bolster network resilience and reliability through precise steering of the reflected beam for RIS. Our approach demonstrates substantial network performance improvements, achieving 95% selection accuracy with only five RC candidates.

REFERENCES

[1] Rafid I. Abd, Daniel J. Findley, and Kwang Soon Kim, "Hydra-RAN Perceptual Networks Architecture: Dual-Functional Communications and Sensing Networks for 6G and Beyond," IEEE Access, vol. 7, pp. 30507–30526, Dec. 2023.

[2] Rafid I. Abd, Daniel J. Findley, and Kwang Soon Kim, " Hydra Radio Access Network (H-RAN): Multi-Functional Communications and Sensing Networks, Initial Access Implementation, Task-1 Approach," IEEE Access, vol. 12, pp. 76532 - 76554, May 2024.

[3] Rafid I. Abd, and Kwang Soon Kim, " Protocol Solutions for IEEE 802.11bd by Enhancing IEEE 802.11ad to Address Common Technical Challenges Associated With mmWave-Based V2X", IEEE Access, vol. 10, pp.100646 - 100664, Sept. 2022.

[4] Rafid I. Abd, and Kwang Soon Kim, "Hydra Radio Access Network (H-RAN): Accurate Estimation Of Reflection Configurations (RCs) for Reconfigurable Intelligent Surfaces (RIS)," in Proc. IEEE 15th International Conference, Conf. Information and Communication Technology Convergence (ICTC), Oct. 2024.

[5] S. Wang, S. Hosseinalipour, V. Aggarwal, Christopher G. Brinton; David J. Love, W. Su, and M. Chiang, "Toward Cooperative Federated Learning Over Heterogeneous Edge/Fog Networks", IEEE Commu. Mag., vol. 61, no. 12, pp. 54 - 60, May 2023.

[6] X. Jia, J. An, H. Liu, and H. Liao, L. Gan, and C.Yuen, "Environment-Aware Codebook for Reconfigurable Intelligent Surface-Aided MISO Communications", IEEE Trans. Wireless Common., vol. 12, no. 7, pp. 1174 - 1178, July 2023.

[7] W. Shen, Z. Qin, and A.Nallanathan, "Deep Learning for Super-Resolution Channel Estimation in Reconfigurable Intelligent Surface Aided Systems", IEEE Trans. Commun., vol. 71, no. 3, pp. 1491 - 1503, March 2023.

[8] M. Almekhlafi, M, Arfaoui, C. Assi, and A. Ghrayeb "A Low Complexity Passive Beamforming Design for Reconfigurable Intelligent Surface (RIS) in 6G Networks", IEEE Trans. on Veh., vol. 72, no. 5, pp. 6309 - 6321, May 2023.

[9] M. Alrabeiah, Y. Zhang, and A. Alkhateeb, "Neural Networks Based Beam Codebooks: Learning mmWave Massive MIMO Beams That Adapt to Deployment and Hardware", IEEE Trans. Commun., vol. 70, no. 6, pp. 3818 - 3833, June 2022.

[10] Q. Xue, Y. Liu, Y. Sun, J. Wang, L. Yan, G. Feng, and S. Ma, "Beam Management in Ultra-Dense mmWave Network via Federated Reinforcement Learning: An Intelligent and Secure Approach", IEEE Trans. on Cognit. Common. and Net., vol. 9, no. 1, pp. 185 - 197, Feb 2023.

[11] Y. Qiao, Y. Niu, X. Zhang, S. Chen, Z. Zhong, N. Wang, and Bo Ai, "Intelligent Beam Management Based on Deep Reinforcement Learning in High-Speed Railway Scenarios", IEEE Trans. on Veh. Tech., vol. 73, no. 3, pp. 3917 - 3931, Mar. 2024.

[12] A. Alkhateeb et al., "Deepsense 6G: A large-scale real-world multimodal sensing and communication dataset", IEEE Commun. Mag., vol. 61, no. 9, pp. 122-128, Sep. 2023.

[13] Remcom, "Wireless insite," [Online]. Available: http://www.remcom.com/wireless-insite.

[14] G. Brockman et al., "OpenAI gym," 2016, arXiv:1606.01540. [Online]. Available:https://arxiv.org/abs/1606.01540.